Superpixel-Based Segmentation of Glioblastoma Multiforme from Multimodal MR Images

Po Su[1,2], Jianhua Yang[1], Hai Li[2], Linda Chi[3], Zhong Xue[2,*], and Stephen T. Wong[2]

[1] School of Automation, Northwestern Polytechnical University, Xi'an, China
[2] Department of Systems Medicine and Bioengineering, The Methodist Hospital Research Institute, Weill Cornell Medical College, Houston, TX
[3] Department of Diagnostic Radiology, MD Anderson Cancer Center, Houston, TX
zxue@tmhs.org

Abstract. Due to complex imaging characteristics such as large diversity in shapes and appearances combining with deformation of surrounding tissues, it is a challenging task to segment glioblastoma multiforme (GBM) from multimodal MR images. In particular, it is important to capture the heterogeneous features of enhanced tumor, necrosis, and non-enhancing T2 hyperintense regions (T2HI) to determine the aggressiveness of the tumor from neuroimaging. In this paper, we propose a superpixel-based graph spectral clustering method to improve the robustness of GBM segmentation. A new graph spectral clustering algorithm is designed to group superpixels to different tissue types. First, a local k-means clustering with weighted distances is employed to segment the MR images into a number of homogeneous regions, called superpixels. Then, the spectral clustering algorithm is utilized to extract the enhanced tumor, necrosis, and T2HI by considering the superpixel map as a graph. Experiment results demonstrate better performance of the proposed method by comparing with pixel-based and the normalized cut segmentation methods.

Keywords: GBM, superpixel, spectral clustering, multimodal MR images.

1 Introduction

Multimodal magnetic resonance (MR) images have been widely used in diagnosis, treatment planning, and follow-up studies of GBM [1] . In multimodal MR scans, GBM often shows a heterogeneous region including an enhanced tumor region, a necrotic region (necrosis), and a non-enhancing T2HI region that is a combination of active tumor cells and possible edema. Accurate segmentation of different tissues of GBM can help neuroradiologists determine tumor margin and assess its progression and aggressiveness. However, due to the complicated imaging characteristics of GBM, such as large diversity in shapes and appearance combining with deformed surrounding tissue, accurate segmentation of GBM from multimodal MR images is challenging.

In the literature, pixel-based automatic segmentation methods [2-5] are widely used. The basic idea is to assign each voxel to a tissue type by considering its

* Corresponding author.

L. Shen et al. (Eds.): MBIA 2013, LNCS 8159, pp. 74–83, 2013.

intensities in multimodal images and the constraints derived from its neighboring pixels or voxels. For example, Clark *et al*. [4] developed a knowledge-based fuzzy clustering algorithm to segment GBM. Prastawa *et al*. [5] considered tumor as outliers of normal tissue, thus the tumor and edema could be isolated by a statistical classification based on learning of intensity distributions for normal brain tissues. Recently, graph cut-based methods [6, 7] have driven more attention. They treat the image as a graph, *i.e.*, pixels as nodes and their similarity as network links or edges. After dividing the graph into sub-networks, the total dissimilarity among different sub-networks and the total similarity within each network are maximized. For example, Corso *et al.* [6] integrated the Bayesian model with graph-based affinities to segment brain tumor from multimodal MR images. However, graph cut-based methods often need to solve a generalized eigenvector problem and may suffer from large computational load when the data set is large. The idea of superpixel [8, 9] can dramatically reduce the number of nodes of the graph and speed up the graph partition while maintaining the image information.

In this paper, we present a superpixel-based graph spectral clustering method for GBM segmentation based on multimodal MR images including T2 weighted (T2), T1 pre-enhanced (T1PRE), T1 post-enhanced (T1POST) and FLAIR. First, a local k-means clustering algorithm with weighted distance is performed to segment the multimodal images into a number of compact and homogeneous superpixels. Then, by considering the brain as a graph of superpixels (*e.g.*, defining nodes as superpixels and links as similarity among superpixels), image segmentation is achieved using spectral clustering of the superpixel network. Compared to the traditional methods, the efficiency and robustness can be improved by using superpixels in the spectral clustering.

In experiments, we first tested the influence of parameters on the segmentation results. Then, we demonstrated the superiority of our method by comparing voxel-based method and standard normalized cut (Ncut) segmentation method.

2 Methods

2.1 Overview

Fig.1. shows the workflow of the proposed method. The pre-processing step consists of skull stripping and co-registration of multimodal images. The FSL [10] skull stripping (BET) and rigid registration (FLIRT) tools are used. In the next step,

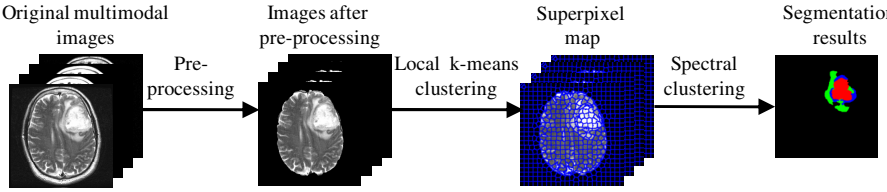

Fig. 1. The workflow of the superpixel-based graph spectral clustering method

superpixels are generated using the local k-means clustering algorithm. Finally, the superpixel-based graph is constructed, and the spectral clustering algorithm is performed to classify the superpixels into different groups, including normal brain tissues, enhanced tumor, necrosis and T2HI.

2.2 Segmenting Images into Superpixels

We used the local k-means clustering algorithm to segment the image into superpixels. In [8], the algorithm was used to generate superpixels from color images. The CIELAB color $[l\ a\ b]$ and the pixel coordinate $[x\ y]$ were used as the image features. A new distance metric d was introduced by simultaneously considering the image features and the size of superpixel:

$$d = \sqrt{{d_f}^2 + \left(\frac{d_{xy}}{S}\right)^2 m^2}, \tag{1}$$

where

$$\begin{aligned} d_f &= \sqrt{(l_i - l_k)^2 + (a_i - a_k)^2 + (b_i - b_k)^2}, \\ d_{xy} &= \sqrt{(x_i - x_k)^2 + (y_i - y_k)^2}, \\ S &= \sqrt{N/K}. \end{aligned} \tag{2}$$

N is the number of pixels, and K is the desired number of approximately equally-sized superpixels. $(l_i, a_i, b_i, x_i, y_i)^T$ represents the 5-D feature of pixel i, and $(l_k, a_k, b_k, x_k, y_k)^T$ is the centroid of the kth cluster, $k \in [1, K]$. d_f measures the color proximity, and d_{xy} measures spatial proximity. m is a parameter that controls the compactness of superpixels, and larger m will induce more compact superpixels. The searching region of the local k-means algorithm is limited to local neighboring region with the size $2S \times 2S$. This results in a significant reduction of computational load over the standard k-means algorithm.

In order to generate superpixels adhering more tightly to the tissue boundaries, we use different weights on T1 post-enhanced image that captures enhanced tumor and necrosis well. Let $[f_{1i}\, f_{2i}\, f_{3i}\, f_{4i}\ x_i\ y_i]$ represents the 6-D feature vector of pixel i, where f_{1i}, f_{2i}, f_{3i}, and f_{4i} represent the image intensities of pixel i located at (x_i, y_i) in T2, T1PRE, FLAIR, and T1POST images, the feature distance between pixel i and the kth cluster center is defined as,

$$d_f = \sqrt{\frac{1-\omega}{3}\sum_{j=1}^{3}\left(f_{ji} - f_{jk}\right)^2 + \omega(f_{4i} - f_{4k})^2}, \tag{3}$$

ω $(0 < \omega < 1)$ is the weight for T1POST image. Fig.2 shows an example of generating superpixels using equally weighted distance $(\omega = 0.25)$ and a higher T1POST weight $(\omega = 0.4)$. In this example, we set $K = 600$, and $m = 70$. We can see that the superpixels generated by using our feature distance adhere better to the boundaries of the enhanced tumor and necrosis (pointed by the red arrows).

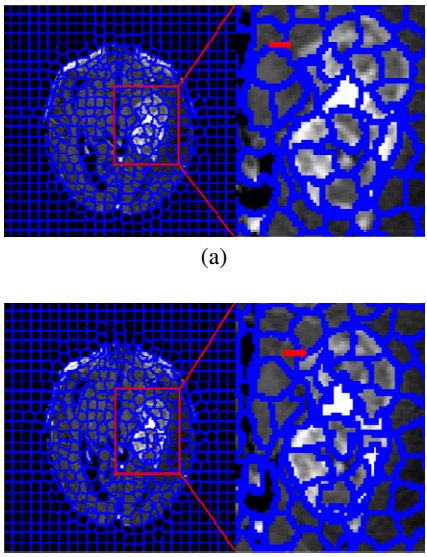

(a)

(b)

Fig. 2. Superpixels generated using standard local k-means clustering and our method. (a) Standard equally weighted; (b) with more weights on T1POST.

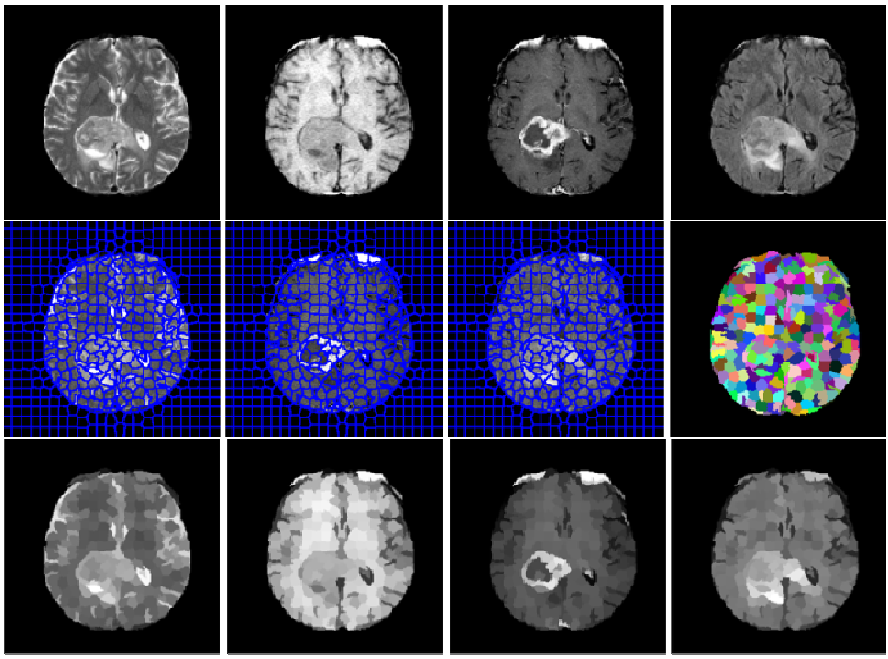

Fig. 3. Examples of superpixel segmentation. Top: original multimodal images (T2, T1PRE, T1POST, and FLAIR); middle: superpixels generated by our method; bottom: superpixels in each modality, from left to right: T2, T1PRE, T1POST, FLAIR.

2.3 Graph Spectral Clustering of Superpixels

After brain pixels are classified into superpixels, with each superpixel consisting of the adjacent pixels with similar multimodal image intensities, we need to further classify them into several major tissue groups. Fig. 3 shows an example of generating superpixels. In the last row, each superpixel is represented by the average intensities in four modalities, and we will use them as features for superpixel classification.

Although the standard k-means clustering algorithm can be used to segment superpixels into enhanced tumor, necrosis and T2HI, it is based on the Euclidean distance to measure the similarity between the superpixels and cluster centroids, and the algorithm is only suitable when data manifold in the feature space is convex. If the data manifold is curved or not convex, the Euclidean distance is inadequate for distinguishing different tissue types. To better handle the similarity and classification of superpixels, the graph partition-based segmentation method is used for superpixel classification. Specifically, for a graph $G = \{V, E\}$ with vertexes $V = \{v_1, v_{2,} \cdots, v_K\}$ representing superpixels, and edge E representing affinity among the superpixels, the affinity of superpixels i and j, w_{ij}, is defined as a Gaussian kernel with width σ,

$$w_{ij} = \exp\left(-\|\mathbf{v}_i - \mathbf{v}_j\|^2 / 2\sigma^2\right). \tag{4}$$

$\mathbf{v}_i$ and $\mathbf{v}_j$ are the average intensity vectors in the four modalities of the vertexes v_i and v_j.

After the superpixel graph is constructed, the graph-based spectral clustering is applied to classify the superpixels into different tissue types. The spectral clustering algorithm [11, 12] reflects the intrinsic data manifolds in the feature space and is suitable for classification of no-convex data. Herein, the normlized spectral clusering algorithm [11] is used. Given the affinity matrix $W = [w_{ij}]$ and the number of the clusters C ($\sigma = 20$, C=6), the following six steps are performed:

1) Define D to be a diagonal matrix with $D_{ii} = \sum_{j=1}^{K} w_{ij}$.
2) Compute the normalized Laplacian matrix $L = D^{-1/2}(D - W)D^{-1/2}$.
3) Compute top C eigenvectors $z_1, z_2, \cdots, z_C$ of L and form the matrix $Z = [z_1\, z_2\, \cdots\, z_C] \in R^{K \times C}$ by stacking the eigenvectors in columns.
4) Form matrix $Y \in R^{K \times C}$ from Z by normalizing the rows to have unit length, *i.e.*, $y_{ij} = z_{ij} / \left(\sum_{c=1}^{C} z_{ic}^2\right)^{1/2}$.
5) Run the k-means clustering to group the row vector Y.
6) Assign the original point v_i to cluster j if and only if row i of the matrix Y is assigned to cluster j.

Finally, the GBM tissue segmentation can be obtained based on the intensity distribution of each group. Fig. 4 shows the sample segmentation results using the spectral clustering algorithm and k-means. For both methods, we set the number of clusters to C= 6. We can see that spectral clustering succeeds to segment all parts of GBM and the results of k-means are not satisfied. Importantly, using the new algorithm, it is much easier to distinguish necrosis with grey matter, as well as T2HI with other white matters.

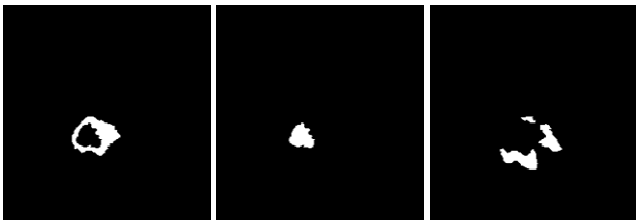

(a)

(b)

Fig. 4. Results using spectral clustering and k-means. (a) Results of spectral clustering. From left to right are enhanced tumor, necrosis, and T2HI; (b) results of k-means clustering.

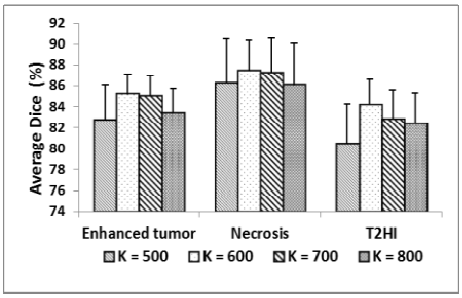

(a)

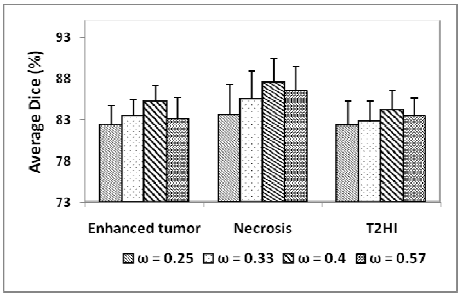

(b)

Fig. 5. The influence of parameter K and ω on GBM tissue segmentation. (a) Segmentation results using different K ($\omega = 0.4$); (b) segmentation results using different ω ($K = 600$).

3 Experiments and Results

Two sets of experiments were conducted to evaluate the performance of our method. The performance of our method relies on superpixels. So in the first experiment, we tested the influence of the parameters on superpixels generation. In the second experiment, we compared our algorithm with voxel-based method [4] and normalized cut (Ncut) [7]. The image data used in the experiments are from 15 patients who have been diagnosed with GBM. For each subject, T2, T1PRE, T1POST and FLAIR images were used with image size of $256 \times 256 \times 21$, and image resolution of $0.78 \times 0.78 \times 6.5\ \mathrm{mm}^3$. The low resolution in z-direction is not suitable for 3D segmentation, so we adopted superpixels to process the images slice-by-slice. The algorithm is extendable for supervoxels for 3D MRI data. The manual marking of GBM tissue by an expert is used as ground truth. Dice similarity score is calculated to evaluate the performance. The Dice similarity score is defined as:

$$Dice(A,B) = \frac{2|A \cap B|}{|A|+|B|}, \tag{5}$$

A represents the pixel sets of GBM tissue of ground truth, B represents the pixel sets of GBM tissue using proposed method or other methods.

3.1 Selection of Parameter

The quality of superpixel segmentation is highly dependent on the choice of parameters: K, m and ω. m controls the compactness of the superpixels and is often set in the range [10,100]. $m = 70$ is adopted in all our experiments, and it offers a good balance between intensity similarity and spatial proximity. To achieve the best segmentation performance, we have tried a range of K and ω. Fig. 5 (a) shows the GBM tissue segmentation results using different K ($\omega = 0.4$). Fig. 5 (b) shows the GBM segmentation results using different ω ($K = 600$). Based on our experiments, we found $K = 600, \omega = 0.4$ can the yield best performance.

3.2 Comparison with other Methods

In the experiment, we applied our method as well as the other two classic segmentation methods, pixel-based method [4] and normalized cut (Ncut) [7] to our image data and compared the segmentation results, both qualitative and quantitative. We found that pixel-based method and Ncut are vulnerable when dealing with complicated cases (GBM with more irregular shape and more heterogeneous intensity). Fig. 6 shows an example of applying the three methods to one subject with complicated GBM characteristics. Fig. 6 (a) and Fig. 6 (b) are the FLAIR and T1POST images of this subject. Fig. 6 (c) is the manually labeled ground truth. Fig. 6 (d) is the result of pixel-based method. Fig. 6 (e) is the result of Ncut. Fig. 6 (f) is the result of our algorithm. From Fig. 6, we can see our method outperform voxel-based method and Ncut on this complicated case.

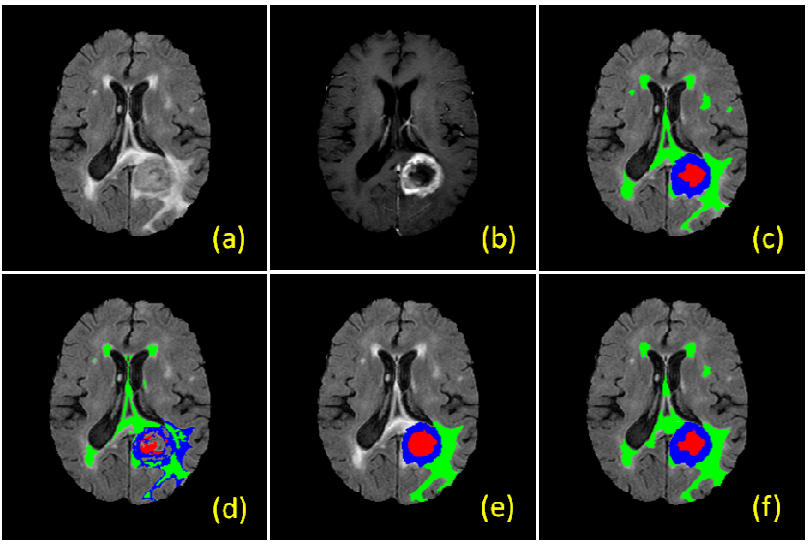

Fig. 6. Comparison of segmentation results on a complicated GBM sample. (a)(b): original FLAIR and T1POST images; (c) groundtruth; (d) pixel-based method; (e) normalized cut; (f) our algorithm. (enhanced tumor: blue region, necrosis: red region, T2HI: green region).

The quantitative results are shown in Fig. 7. We can see that our algorithm is more accurate. Pixel-based segmentation method does not take local or global spatial information into account and easily generate unsatisfied segmentations when the intensity of GBM tissues overlaps each other. For Ncut, it can yield good results when the shape of GBM tumors are compact and regular, when the shape of GBM is irregular and complicated, this method is limited (see Fig. 6 (e)). Furthermore, Ncut needs to solve a generalized eigenvector problem, when the image size is large, it suffers high computational load. Compared with other two methods, our algorithm combines the advantages of superpixel and spectral clustering is more suitable for GBM segmentation.

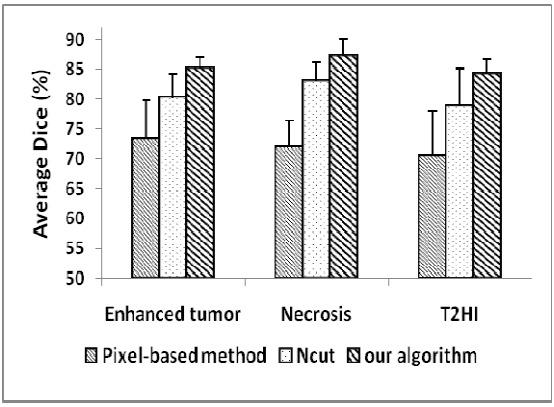

Fig. 7. Comparison of our algorithm with pixel-based and Ncut methods

4 Conclusion

We developed a superpixel-based graph spectral clustering algorithm that combines superpixel and graph spectral clustering to segment GBM from multimodal MR images. The basic idea is that the superpixel method groups spatially relate pixels with similar intensities together, and the graph spectral clustering on superpixels reduces the computational load and improves the accuracy of the segmentation. Comparative study showed the proposed method can achieve more accurate results. Because the z-direction resolution of our image data is very low, we used superpixel instead of supervoxel. It can be easily extended to use supervoxel for 3D scans. Quantitative segmentation of GBM from multimodal images provides detailed diagnostic information. For example, the shape and size of the enhanced tumor, necrosis, the region of T2 hyperintensity (T2HI), the intensity distribution within each region, as well as the transition from enhanced tumor to T2HI may provide important information about the aggressiveness of GBM. In the future, we plan to extract these features and correlate with the pathological finding aiming at providing more quantitative diagnostic measures for GBM subtyping and aggressiveness assessment.

References

1. Petrella, J.R., Provenzale, J.M.: MR perfusion imaging of the brain: techniques and applications. American Journal of Roentgenology, 207–219 (2000)
2. Constantin, A.A., Bajcsy, B.R., Nelson, C.S.: Unsupervised segmentation of brain tissue in multivariate MRI. In: 2010 IEEE International Symposium on Biomedical Imaging: From Nano to Macro, pp. 89–92. IEEE (2010)
3. Fletcher-Heath, L.M., Hall, L.O., Goldgof, D.B., Murtagh, F.R.: Automatic segmentation of non-enhancing brain tumors in magnetic resonance images. Artificial Intelligence in Medicine 21, 43–63 (2001)
4. Clark, M.C., Hall, L.O., Goldgof, D.B., Velthuizen, R., Murtagh, F.R., Silbiger, M.S.: Automatic tumor segmentation using knowledge-based techniques. IEEE Transactions on Medical Imaging 17, 187–201 (1998)
5. Prastawa, M., Bullitt, E., Ho, S., Gerig, G.: A brain tumor segmentation framework based on outlier detection. Medical Image Analysis 8, 275–283 (2004)
6. Corso, J.J., Sharon, E., Dube, S., El-Saden, S., Sinha, U., Yuille, A.: Efficient multilevel brain tumor segmentation with integrated bayesian model classification. IEEE Transactions on Medical Imaging 27, 629–640 (2008)
7. Shi, J.B., Malik, J.: Normalized cuts and image segmentation. IEEE Transactions on Pattern Analysis and Machine Intelligence 22, 888–905 (2000)
8. Achanta, R., Shaji, A., Smith, K., Lucchi, A., Fua, P., Susstrunk, S.: SLIC superpixels compared to state-of-the-art superpixel methods. IEEE Trans. Pattern Anal. Mach. Intell. 34, 2274–2282 (2012)
9. Lucchi, A., Smith, K., Achanta, R., Knott, G., Fua, P.: Supervoxel-based segmentation of mitochondria in EM image stacks with learned shape features. IEEE Trans. Med. Imaging 31, 474–486 (2012)

10. Smith, S.M., Jenkinson, M., Woolrich, M.W., Beckmann, C.F., Behrens, T., Johansen-Berg, H., Bannister, P.R., De Luca, M., Drobnjak, I., Flitney, D.E.: Advances in functional and structural MR image analysis and implementation as FSL. Neuroimage 23, 208 (2004)
11. Ng, A.Y., Jordan, M.I., Weiss, Y.: On spectral clustering: Analysis and an algorithm. In: Advances in Neural Information Processing Systems, pp. 849–856 (2001)
12. Von Luxburg, U.: A tutorial on spectral clustering. Statistics and Computing 17, 395–416 (2007)